ABUAD Journal of Engineering Research and Development (AJERD)
ISSN: 2645-2685

Volume 3, Issue 2, 54-65

Cyanide Biosorption from Aqueous Solution by Iron-impregnated Palm Kernel Fibre Adsorbent: Equilibrium, Kinetics and Optimization

Michael Sunday OLAKUNLE[1], Olusegun Ayoola AJAYI[1], Francisca Unoma NWAFULUGO[2]

[1]*Department of Chemical Engineering, Ahmadu Bello University, Zaria, Nigeria*
msolakunle@abu.edu.ng/oaajayi@abu.edu.ng

[2]*Federal Polytechnic, Oko, Anambra State, Nigeria*
francaunoma@yahoo.com

Corresponding Author: molakunles@gmail.com

Date Submitted: 26/08/2020
Date Accepted: 26/09/2020
Date Published: 31/12/2020

Abstract: *Cyanide poisoning in water bodies often results from human activities via cassava processing, which is highly undesirable in water bodies. This work describes the preparation of palm kernel fibre ash (PKFA) adsorbent via wet beneficiation, calcination and impregnation with Iron (II) nitrate for cyanide adsorption from its aqueous solution. The raw palm kernel fibre (PKF), calcined PKFA and Fe^{2+} impregnated PKFA (Fe-PKFA) were characterized using a scanning electron microscope (SEM) and Fourier Transform Infrared (FTIR), whereas UV spectrophotometer was used to monitor the cyanide concentration. Box-Behnken experimental design method of the response surface methodology (RSM) was employed to study the effect of temperature, contact time, adsorbent dosages, and initial concentration on the adsorption efficiency of the adsorbents at fixed pH 7. Optimal adsorption efficiency of 85.43% was obtained with 60 ppm initial concentration, 3 g of calcined Fe-impregnated adsorbent dosage at 42 minutes contact time and temperature of 35 ^oC. The developed model for the adsorption process gave R^2 value of 0.9985 which shows that the model is significantly high, and there was good agreement between the experimental and simulated values. The adsorption process was best described by the pseudo-second order and intra particle diffusion kinetic models. The Temkin adsorption isotherm gave the highest regression coefficient and the variation of adsorption energy was 14.47kJ/mol which indicated an exothermic process. The results revealed that the Fe^{2+} impregnated PKFA adsorbent can serve as a good and sustainable adsorbent for cyanide biosorption from wastewater.*

Keywords: Biosorption, adsorbent, palm kernel fibre ash, cyanide, response surface methodology.

1. INTRODUCTION

Cassava processing effluent in concentrated industrial areas is often regarded as polluting and a burden on natural resources. Processing of cassava for starch is water-intensive and generates large volumes of wastewater (between 7 m^3 per kg to about 69 m^3 of wastewater per ton of fresh cassava roots), [1,2]. In Nigeria, between 20–60 m^3 per ton of cassava wastewater generated during cassava processing [3-5], find their way into nearby drains and streams, causing critical health-threatening pollution to the waterbody. The wastewater is highly acidic, sometimes as low as pH of 2.6, and combined wastewater has been reported as ranging between pH of 3.5 and 5.2 [6], which causes harm to aquatic organisms and prevent self-purification of the receiving water body [7]. These wastes would even be more problematic in the future with the increased industrial production of cassava products. The Food and Agricultural Organization (FAO) reported that of the total world production of cassava in 2000, Africa accounted for 54%, Asia 28%, Latin America and Caribbean 19%. In 1999, Nigeria produced 33 million tons of cassava, with the figure rising to 184 million tons in 2002, making it the world's largest producer [5, 7-10].

Hydrocyanic acid (HCN) or cyanide is a major poisonous chemical substance present in a deadly concentration in raw cassava tuber [11, 12]. The cyanide content per peeled tubers varies from 6 to 250 mg $HCNkg^{-1}$ fresh weight, with a reported maximum of 434 mg $HCNkg^{-1}$. Presence of 50 mg $HCNkg^{-1}$ fresh weight is regarded as nontoxic [6], but higher than that is toxic, [13]. According to Burns *et al.* [14], cyanide in cassava exists in the form of glycoside, (i.e. linamarin and lotaustralin), which is easily liberated from cassava cyanogenic glycosides by the enzyme linamarase.

The current technologies used for cyanide effluents treatment like anodic oxidation, electrical attenuation, biodegradation etc. [15-18] are inadequate due to the quantity of these wastes. The biodegradation method often leads to the problems of metal-bearing sludge which are difficult to dispose. Some of these traditional methods are expensive thereby proving uneconomical, especially for developing countries where large volumes of these waste are generated [19]. Therefore, there is a need for newer and effective methods which will also be efficient and cheap. Compared with conventional methods for removing toxic metals from effluents, the biosorption process has the advantage of the ease and low operating cost, high removal capacity, minimization of volume of chemicals and biological sludge to be disposed of and high efficiency in detoxifying very dilute effluent [20, 21].

Adsorbents produced from agricultural by-products has been given serious attention due to the growing interest in low-cost adsorbent from renewable biomass, especially for applications in the treatment of wastewater [22, 23]. According to Herawan *et al.* [24], two major solid wastes are generated during palm oil processing, which includes, the extracted flesh fibre (mesocarp) and seed shell (endocarp). Poku [25], also reported that during oil palm processing, about 20-24% of fresh fruit bunch (FFB) are converted to oil, while the remaining 76-80% are essentially waste-products. The oil palm industry generates a high amount of the palm kernel fibre (PKF) from its operation, which if not properly disposed of could pose an environmental problem, [26-28]. Anyanwu [29] and Ohimain *et al.*, [30], in their separate surveys, revealed that an average of 382,500 dry tons of PKF is generated in Nigeria annually.

The potential of palm kernel fibre (PKF) as a low-cost biosorbent material has been receiving interest in recent researches [31, 32]. Oil-palm fibre is a good candidate for advanced material production because they are available as wastes, which could be gotten almost free in small quantity or low price in huge quantity [24]. Palm kernel fibre ash (PKFA) has been reported to have about 66.64% amorphous content with silicon dioxide (SiO_2) as the main constituent, [33]. In this study, adsorbent preparation from PKF, impregnated with iron (II) nitrate for cyanide removal from aqueous solution and their removal efficiency using numerical optimization technique in Box-Behnken method of the response surface methodology was investigated. Also, data obtained from the design expert software for the adsorption study was used to carry out both the kinetics and isotherm studies.

2. MATERIALS AND METHOD

2.1 Materials

The raw palm kernel fibre (PKF) was sourced from a palm oil industry in Esit-Eket Local Government Area in Akwa Ibom State, Nigeria, having latitude 4.6607^0 N, longitude 8.0683^0 E. Analytical grade (Sigma-Aldrich, Germany) potassium cyanide (KCN), ACS reagent ≥ 96.0%, Iron (II) Nitrate ($Fe(NO_3)_2$) and deionized water were used for the preparation of the stock solution for the adsorption study, and impregnation of the palm kernel fibre ash.

2.2 Preparation of the Cyanide Standard Solution

1 g of potassium cyanide (KCN) was dissolved in 1000 ml of de-ionized water to prepare a stock solution of KCN. 10 to 60 ppm cyanide concentrations were prepared from the stock solution in steps of 10 ppm by serial dilution. Perkin Elmer LAMBDA 265 UV spectrophotometer set at 600 nm was used to generate a calibration curve using the six-prepared solution and a blank solution [34]. The linear Beer-Lambert relationship between absorbance and cyanide concentration for the calibration curve was established by plotting these parameters and observing the regression. Subsequent determination of unknown concentrations was determined using the model developed from the regression.

2.3 Sample Pre-treatment and Calcination.

The raw palm kernel fibre was beneficiated by soaking in hot deionized water and detergent for 24 hours to remove the associated oil. The remaining debris was removed by thorough rinsing in hot deionized water, air-dried and carbonized for 72 hours in a rotary kiln [35]. The carbonized PKF was washed in water, filtered, sieved to a particle size of 250 microns and left to settle for a day in a quiescent condition. The resulting slurry was oven-dried at 80 °C for 6 hours, ball-milled to powdered form and then calcined in a muffle furnace at 550 °C overnight followed by further heating at 750 °C for 1 hour. The ASTM E871, ASTM D1102 and ASTM E872 [36] methods were used to conduct the proximate analysis for the palm kernel fibre.

2.4 Impregnation with Iron (II) Nitrate

The wet impregnation method was used to anchor the iron on the PKFA. 5 g of iron (II) nitrate was dissolved in 480 ml of deionized water to form a solution. 50 g of the calcined PKF ash was introduced into the iron (II) nitrate solution and

stirred for 2 hours. The resulting slurry was aged for 24 hours before it was oven-dried at 80 ºC for 6 hours and later calcined at 450 ºC. The various stages of all the transformation were characterized using SEM and FTIR.

2.5 Batch Adsorption Experiment and Optimization Studies.

25ml solution each of (25–60 ppm) of KCN at the time (6–42 minutes) and temperature of (30–40 ºC) in a 100 ml batch reactor were contacted with the Fe^{2+}-impregnated PKFA adsorbent (1–5 g), in a batch adsorption experiment. The specific combinations were as suggested by the Box-Benkhen method of design of experiment (Design-Expert v11 software, Stata-Ease Inc.). The optimum conditions for maximum adsorption of cyanide by Fe-PKFA was determined using a four-factor, Box-Behnken experimental design combining with response surface methodology. This work focuses on the design of four factors (temperature, contact time, ash dosage and initial concentration of cyanide) to determine the optimum adsorption conditions, using percentage cyanide removal as a response, as depicted in Table 1. The concentration of cyanide after adsorption was determined using Perkin Elmer LAMBDA 265 UV spectrophotometer. The cyanide removal percentage was calculated using Equation 1:

$$R(\%) = \frac{C_o - C}{C_o} \times 100 \qquad 1$$

where R = Removal Efficiency, C_0 = Initial Concentration of Cyanide, ppm, C = Final Concentration of Cyanide, ppm

3. RESULTS AND DISCUSSION

3.1 Scanning Electron Microscope (SEM) Analysis

Plate 1 shows the surface morphology of raw PKF, carbonized PKFA and the Fe-impregnated PKFA. It demonstrates the changes in surface morphology from the raw PKF to the Fe-impregnated PKFA. It could be seen from plate 1a that the raw palm kernel fibre is a bundle of many fibres, which indicates that these vessel elements are nothing but individual fibres.

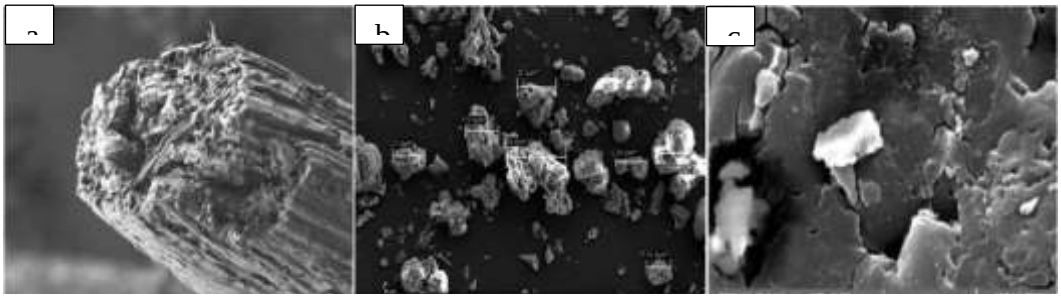

Plate 1: SEM morphological images for (a) raw PKF (b) carbonized PKFA and (c) calcined Fe^{2+}-impregnated PKFA

The raw fibres have a smooth and homogenous surface with highly well-developed porous texture as corroborated by Abdelwahab *et al.*, [37] and Tobi *et al.*, [38]. On carbonization, the fibre bundle was broken into a relatively smooth solid structure with the formation of several pores on its surface (Plate 1b). The carbonized PKFA surface was also covered with silica, [39-41], while this silica may decrease the number of the adsorbed particle due to the adsorbate that cannot enter. It can be seen in Plate 1c, that the impregnated iron particles (brighter and small aggregates form) are inside the porous structure and on the surface of the carbonized PKFA due to the impregnation process. This was found to conform to the works reported by Depci, [42]. The results revealed that treatment of the carbonized PKFA with $Fe(NO_3)_2$ successfully modified the PKFA outer layer surface by developing several new pores due to the loss of volatile components to form a highly porous structure.

3.2 Fourier Transform Infrared Spectrometry (FTIR)

Figures 1a, b and c reveal the FTIR spectra of raw PKF, carbonized PKFA and calcined Iron impregnated PKFA. The shift in peak values as could be seen across the FTIR images are due to the formation of a chemical bond between functional groups present on the adsorbents. Based on the FTIR, confirmation of potential application for adsorption can be deduced with good removal efficiency.

In the diagnostic domain, the transmittance pattern of the infrared light helps to determine the functional group present in the samples. It could be seen that the spectra have similar peaks for all the samples with slight variations. A broad and strong peak could be noticed at 3424 cm^{-1} on the spectra, which corresponds to the hydroxyl (-OH) group stretching [38]. From Figure 1a, the peak at 628.81 cm^{-1} bandwidth fall in the Infra-red (IR) band range of (1000–650) cm^{-1} and the functional

group present was C-H alkenes out-of-plane bend. Peak having 1643.41 cm^{-1} bandwidth reveals the presence of C=C of amide functional group for an IR band range of (1670–1640) cm^{-1} bandwidth as could be seen in Fig. 1a and b. For the carbonized PKFA, the peak at 2870.17 cm^{-1} bandwidth and 2933.83 cm^{-1} bandwidth indicates the presence of (C-H) alkanes stretch as it falls in the IR range of (3000–2850) cm^{-1} as corroborated by Tobi *et al.*, [38]. The peak at 1041.6 cm^{-1} and 1107 cm^{-1} which fall in an IR band range of (1300–1000) cm^{-1} of Figure 1b and 1c identify the presence of C-C functional groups.

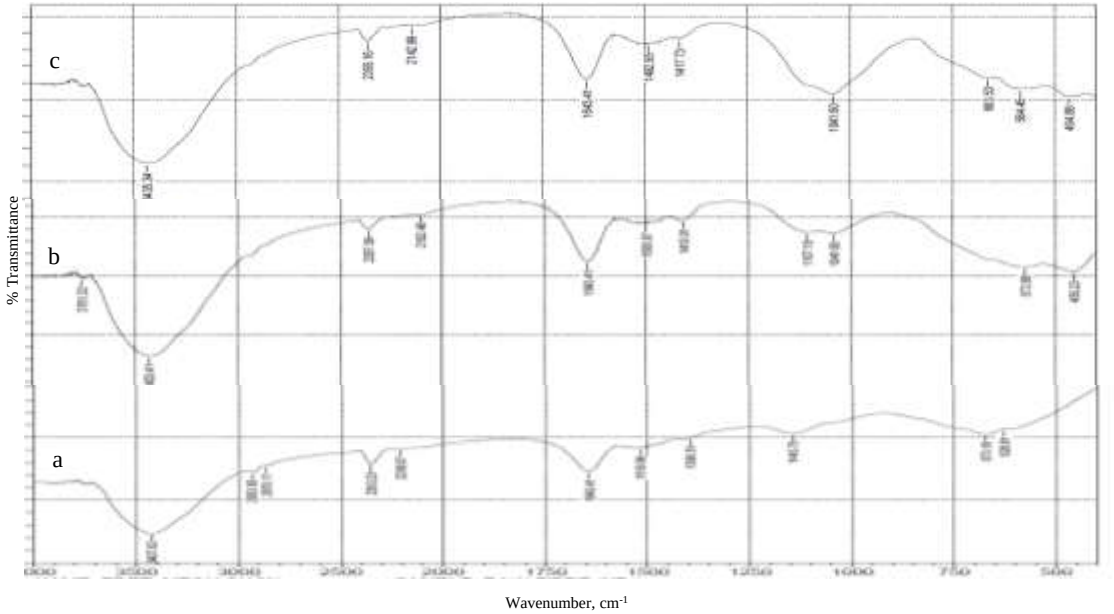

Figure 1: FTIR Spectra of (a) raw PKF, (b) carbonized PKFA, (c) Fe^{2+} impregnated PKFA

The change in FTIR spectra confirms the effect of Iron impregnation on raw ash; also, the shift in spectra shows that palm fibre will be a useful adsorbent for cyanide treatment. Figure 1b and 1c, by comparison, reveals mostly that alkanes and amides will be involved in the adsorption process. There were clear bandwidth shifts and intensity decrease at 464.86 cm^{-1}, 584.45 cm^{-1}, 663.53 cm^{-1}, 1492.95 cm^{-1} and 2142.99 cm^{-1} bandwidth. The broad O-H stretching vibration mode at 3400 cm^{-1} which suggests the presence of hydroxyl groups provide a hydrophilic component to Fe^{2+}, increasing their dispersibility [43]. The other bands below 800 cm^{-1} are attributed to the blending metal-oxygen stretching modes, including Fe-O originating from $Fe(NO_3)_2$.

3.3 Batch Adsorption Experimental Study

Table 1 shows the results of the Box-Behnken design of experiment. The removal efficiency of the cyanide was seen to vary between 77.22% and 87.89% for the experimental values. The error range when compared with the predicted values are within acceptable limit (-0.19 to +0.2). The regression analysis done enhances the developed model that was used to study the analysis of variance resulting from the graph and parity plots.

Table 1: Experimental Design Matrix with Response.

Run	A: Temperature degree C	B: Contact Time, minutes	C: Ash Dosage, g	D: Initial Concentration, ppm	Removal Efficiency, %	
					Experimental Value	Predicted Value
1	35	6	3	60	80.22	80.16
2	35	24	3	42.5	84.49	84.46
3	35	24	3	42.5	84.3	84.46
4	35	24	5	25	83.96	83.81
5	40	24	5	42.5	87.48	87.37
6	35	6	3	25	79.19	79.34
7	35	24	5	60	84.26	84.31
8	30	6	3	42.5	78.96	78.86
9	35	24	1	60	81.43	81.57
10	35	24	3	42.5	84.63	84.46

11	30	24	3	60	83.51	83.54
12	40	24	3	25	86.62	86.57
13	35	24	3	42.5	84.43	84.46
14	30	24	3	25	82.96	82.99
15	40	24	3	60	87.26	87.21
16	35	6	1	42.5	77.22	77.07
17	35	42	5	42.5	85.28	85.40
18	30	24	5	42.5	83.46	83.43
19	35	42	3	60	85.53	85.43
20	35	42	3	25	84.96	85.06
21	30	24	1	42.5	80.76	80.91
22	35	24	1	25	80.94	80.87
23	35	6	5	42.5	80.13	80.24
24	40	6	3	42.5	83.28	83.33
25	35	42	1	42.5	83.04	82.90
26	40	42	3	42.5	87.89	87.98
27	35	24	3	42.5	84.45	84.46
28	30	42	3	42.5	85.27	85.20
29	40	24	1	42.5	84.15	84.22

1). Analysis of Variance (ANOVA): Table 2 shows the ANOVA of the cyanide removal which influenced the model development. Statistically, if the prob > F value is less than 0.05, the model developed is said to be significant. Also, for lack of fit not to be significant, the prob > F value must be greater than 0.1.

Table 2: Summary of Analysis of Variance (ANOVA)

Source	**Sum of Squares**	**df**	**Mean Square**	**F-value**	**p-value**	
Model	196.69	14	14.05	673.31	< 0.0001	Significant
A-Temperature	39.46	1	39.46	1891.02	< 0.0001	
B-Contact Time	90.59	1	90.59	4341.26	< 0.0001	
C-Ash Dosage	24.17	1	24.17	1158.26	< 0.0001	
D-Initial Conc.	1.07	1	1.07	51.19	< 0.0001	
AB	0.7225	1	0.7225	34.63	< 0.0001	
AC	0.0992	1	0.0992	4.76	0.0468	
AD	0.0020	1	0.0020	0.0970	0.7600	Not significant
BC	0.1122	1	0.1122	5.38	0.0360	
BD	0.0529	1	0.0529	2.54	0.1337	Not significant
CD	0.0090	1	0.0090	0.4325	0.5214	Not significant
A^2	6.23	1	6.23	298.55	< 0.0001	
B^2	16.58	1	16.58	794.57	< 0.0001	
C^2	13.76	1	13.76	659.24	< 0.0001	
D^2	0.8642	1	0.8642	41.41	< 0.0001	
Residual	0.2921	14	0.0209			
Lack of Fit	0.2357	10	0.0236	1.67	0.3276	Not significant
Pure Error	0.0564	4	0.0141			
Cor Total	196.98	28				
R^2	0.9985					
Adjusted R^2	0.9970					
Predicted R^2	0.9927					
Adeq Precision	104.9805					

Thus, as shown in Table 2, the Model F-value of 673.31 implies the model is significant and its corresponding prob > F value obtained to be 0.0001 is less than 0.05 which implies that there is only a 0.01% chance that a "Model F-value" this large could occur due to noise. The Lack of Fit F-value **o**f 1.67 implies the Lack of Fit is not significant relative to the pure error. There is a 32.76% chance that a "Lack of Fit F-value" this large could occur due to noise. Non-significant lack of fit

is good. The model terms are A, B, C and D. In this case from Table 2, A, B, C, D, AB, AC, BC, A^2, B^2, C^2, D^2 are significant model terms. Values greater than 0.1000 indicate the model terms are not significant. Eliminating the insignificant model terms we have;

$$\text{Removal Efficiency}, \% = 84.46 + 1.81A + 2.75B + 1.42C + 0.2983D - 0.425AB + 0.1575AC - 0.1675BC + 0.98A^2 - 1.6B^2 - 1.46C^2 - 0.365D^2 \quad \ldots(2)$$

where A, B, C and D represent temperature, ash dosage, contact time and initial concentration of cyanide respectively.

Equation 2 represents the model developed for cyanide removal. As can be seen from Equation 2, it represents a polynomial model of quadratic order which can be used to predict cyanide removal before laboratory experiment. The contribution of term B (contact time) is more significant judging from the value of its coefficient, whereas the AC term indicates the most effective interrelated combined quadratic factors. The model in terms of actual factors is as presented in Equation 3 in the light of the significant factors as shown in Table 2.

$$\text{Removal Efficiency} = 102.18769 - 2.32618T + 0.584243CT + 2.51205AD + 0.122187IC - 0.004722T*CT + 0.015750T*AD - 0.004653CT*AD + 0.039200(T)^2 - 0.004934(CT)^2 - 0.364063(AD)^2 - 0.001192(IC)^2 \quad \ldots3$$

where T = temperature, CT = contact time, AD = ash dosage, and IC = initial concentration

The equation in terms of actual factors can be used to make predictions about the response for given levels of each factor. Here, the levels should be specified in the original units for each factor. This equation should not be used to determine the relative impact of each factor because the coefficients are scaled to accommodate the units of each factor and the intercept is not at the centre of the design space.

The Predicted R^2 of 0.9927 is in reasonable agreement with the Adjusted R^2 **o**f 0.9970; i.e., the difference is less than 0.2. The R^2 value of 0.9985 indeed showed that the model is significantly high, and there was good agreement between the experimental and simulated values.

2) Relationship between the predicted and actual data: Figure 2 shows the parity plot of the apredicted and actual data in the model development. As shown in Figure 2, both experimental (actual) and predicted data are very close to the regression line which proves that the experimental data are in close agreement with the predicted data. This shows that there is a very good correlation between the data points [44, 45]. This is evident in the R^2 value of 0.9985 obtained which is close to 1.0 as desired in regression analysis.

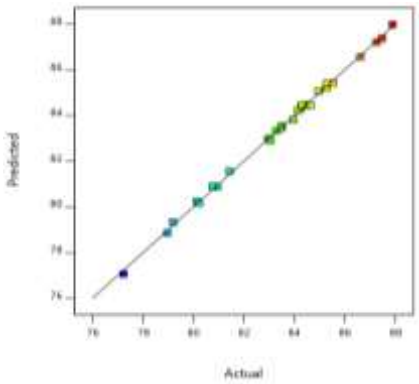

Figure 2: Parity plot of the predicted and actual data

3) Response Surface Plot: The response surface plot shows the relationship between the variable parameters used and their corresponding responses. Figures 3(a) and (b) follows the same trend, indicating that the combined effect of Ash dosage (C) and contact time (B) respectively with temperature both leads to higher removal of the cyanide as their values increase. Figure 3(a) showed that higher temperature favoured high removal of the cyanide ion. However, operating at higher temperature >37 ^{0}C may come with higher energy cost implication, whereas the % removal at 35 ^{0}C will also yield not too different removal efficiency. Higher temperature above 36 ^{0}C and higher ash dosage is certainly not economical for the process

As shown in Figure 3(b), at a temperature of 30 ^{o}C and contact time of 42 minutes, the cyanide removal efficiency amounted to about 89 %. When the temperature is increased to 36 ^{o}C at the reduced contact time, there was a reduction in cyanide removal efficiency. It can, therefore, be inferred that lower temperature and longer contact time will bring about better performance in terms of the cyanide removal by the adsorbent. This is in line with the work previously reported by Kumar *et al.* [46].

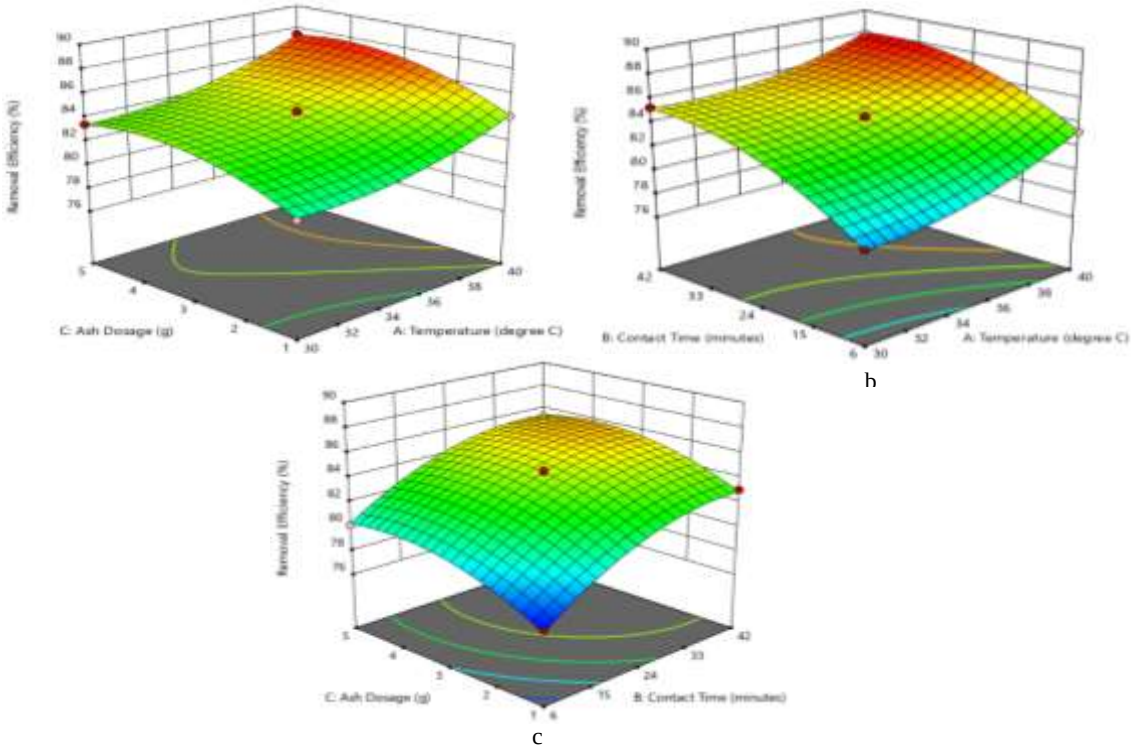

Figure 3: Effect of Temperature (A), Contact Time(B) and Ash Dosage (C) on cyanide removal efficiency

Higher removal efficiency is also observed as contact time increases with ash dosage up to a contact time of about 24 minutes with a corresponding ash dosage of 3g, which gave a removal efficiency about 84.49% (see Figure 3(c)). Contact time above 24 minutes and corresponding increase or decrease of ash dosage will result in reduced removal efficiency.

4) Optimization Point of Design of Experiment (DOE) Software: Optimization of the variables was carried out using numerical optimization tool of the response surface methodology of the design of experiment software. Table 3 gives the selected experimental variables to attain desirable results from those obtained after laboratory work.

Table 3: Selected Experimental Variables by DOE.

S/N	Temperature	Contact Time, mins	Ash Dosage, g	Initial Concentration, ppm	Removal Efficiency, %	Desirability	
1	35.000	42.000	3.000	60.000	85.427	1.000	Selected
2	30.000	24.000	3.000	60.000	83.537	1.000	
3	**40.000**	**24.000**	**3.000**	**60.000**	**87.209**	**1.000**	
4	35.000	24.000	5.000	60.000	84.309	1.000	
5	35.000	24.000	1.000	60.000	81.565	1.000	
6	39.585	17.021	4.726	60.000	86.071	1.000	

Operating at any selected values in Table 3 will result in better adsorption efficiency as can be observed from desirability since all have the same desirability. As seen on Table 3, the design of experiment software suggested an optimal cyanide removal of 85.43 % at a temperature of 35 ^{o}C, ash dosage of 3 g, initial cyanide concentration of 60 ppm and a contact time of 42 minutes. However, a higher removal of 87.21% can be achieved at an optimal condition of 40 ^{0}C, 24 minutes contact time, 3 g ash dosage and 60 ppm initial cyanide concentration. This could be justified by the fact that higher removal is

achieved in lesser contact time, which is compensated by higher temperature. Thus, the cost of achieving higher purity in less time could be compensated by a little rise in temperature as compared to the suggested values by the software.

5) Adsorption Kinetics and equilibrium modelling: The applicability of kinetic models i.e. zero, pseudo-first, pseudo-second order and intra particle diffusion were investigated by measuring the regression coefficients. As depicted in the Figures 4(a-d), pseudo-second order and intra particle diffusion model best described the adsorption process. This implied that the adsorption involved chemisorption [47] at a high rate of diffusion of the adsorbate [48] with low mass transfer resistance on the adsorbent [49], having an impressive adsorption rate as depicted in Table 4. The value of the q_t does not correlate linearly with *t*, hence intra particle diffusion process could not be the rate limiting step. Accordingly, it can be concluded that the adsorption of cyanide on iron impregnated palm kernel fibre is simultaneously governed by liquid diffusion, intra particle diffusion and chemical surface sorption process.

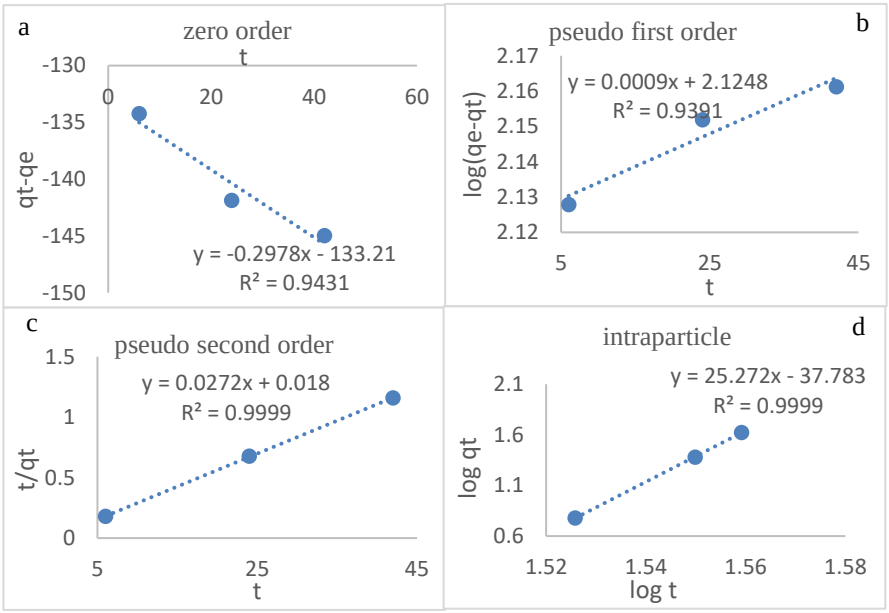

Figure 4: Kinetics modelling of cyanide adsorption by Fe^{2+}-PKFA adsorbent

Table 4: Adsorption kinetic parameters of various kinetic models

Kinetic models	Adsorption Parameters		
Zero-order	R^2=0.9431	K_0=0.2978 min^{-1}	Q_e=133.21
Pseudo-first order	R^2=0.9391	K_1=0.0021 min^{-1}	Q_e=133.29
Pseudo-second order	R^2=0.9999	K_2=0.0411 g/mg/min	Q_e=36.76
Intraparticle	R^2=0.9999	K_T=6.067E03 mg/g/$min^{0.5}$	

To establish the affinity of cyanide on the adsorbent, Langmuir, Dubinin-Radushkevich (D-R), Freundlich and Temkin isotherm were used to analyse the data obtained from the sorption process. The graphical representation of all the isotherm models are displayed in Figure 5(a-d). Ironically, all the isotherms have relatively high regression coefficient, pointing to the complexity of the adsorption process.

The E value for D-R model corroborate the chemical adsorption, depicted by the kinetic model as stated earlier. The low regression coefficient for Langmuir and D-R suggest that mode of adsorption is not heterogeneous in nature and confirms the surface homogeneity of the adsorbent. The separation factor (R_n) obtained to be 0.023 indicated that adsorption of cyanide on Fe^{2+}-PKFA is a favourable process, which corroborate with high Freundlich exponent n-factor.

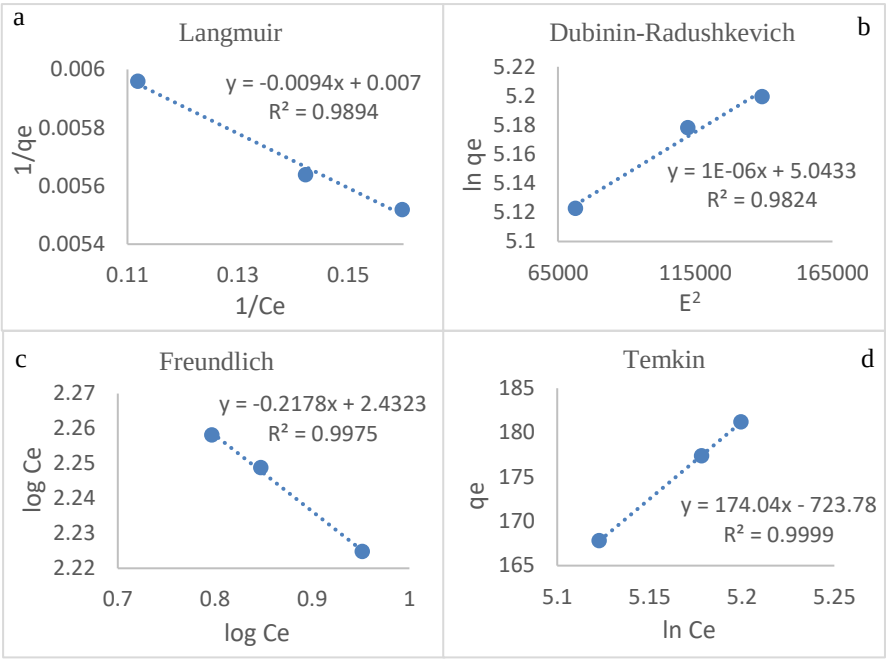

Figure 5: Equilibrium modelling of cyanide adsorption by Fe^{2+}-PKFA adsorbent

Table 5: Equilibrium parameters for Cyanide adsorption by Fe^{2+}-PKFA Adsorbent

Two-Parameter Isotherm Model				
Langmuir	R^2 = 0.9894	K_L=0.7194 L/mg	Q_m = 147.86 mg/g	R_L = 0.023
Dubinin-Radushkevich	R^2 = 0.992	Q_m=138.13 mg/g	B = 0.0007 J/mol	E = 26.72 kJ/mol
Freundlich	R^2 = 0.9975	K_F=11.39 L/mg	N = 4.5914	
Temkin	R^2 = 0.999	K_T=63.99 L/g	B = 14.47 kJ/mol	

It could be observed from Table 5 that Temkin isotherm gave the highest regression coefficient. The variation of adsorption energy in Temkin model (B) was 14.47kJ/mol indicating that the process is exothermic which was in agreement with the works of Shahbeig *et al.*, [50] and Chan *et al.* [51].

4. CONCLUSION

Palm Kernel Fibre considered to be waste was beneficiated, thermally treated and chemically modified to improve its property needed for cyanide adsorption. The various characterizations of the palm kernel fibre prove the potential of its applicability. The iron impregnated palm kernel fibre ash was able to adsorb cyanide from the synthesized wastewater and response surface methodology was used to determine the optimal adsorptive efficiency at varying operating conditions of cyanide concentration, dosage of calcined Fe-impregnated PKFA, contact time and temperature. Optimal values of 60 ppm, 3 g, 24 minutes and 40 ^{0}C respectively yielded a removal efficiency of 87.209 % cyanide removal. Pseudo-second order and intra particle diffusion kinetics well described the adsorption process, and the Temkin adsorption isotherm gave a 14.42 kJ/mol adsorption energy released by the process.

REFERENCES

[1] Cappelletti, B.M., Reginatto, V., Amante, E.R. and Antônio, R.V. (2011). Fermentative production of hydrogen from cassava processing wastewater by *Clostridium acetobutylicum*. *Renewable Energy* 36(12): 3367-3372. https://doi.org/10.1016/j.renene.2011.05.015

[2] Ugwu, E.I. and Agunwamba, J.C. (2012). Detoxification of cassava wastewater by alkali degradation. *Journal of Research in Environmental Science and Toxicology*: 1(7) pp. 161-167. (ISSN: 2315-5698)

[3] Oboh, G. (2006). Nutrient enrichment of cassava peels using a mixed culture of *Saccharomyces cerevisiae* and *Lactobacillus spp* solid media fermentation techniques. *Electronic Journal of Biotechnology* 9(1): 46-49. ISSN: 0717-3458

[4] Afuye, G.G. and Mogaji, K.O. (2015). Effect of cassava effluents on domestic consumption of 'shallow well' water in Owo Local Government Area, Ondo State, Nigeria. *Physical Sciences Research International,* 3(3): 37-43. ISSN: 2437-1300

[5] Oghenejoboh, K.M. (2015). Effects of Cassava Wastewater on the Quality of Receiving Water Body Intended for Fish Farming. *British Journal of Applied Science & Technology* 6(2): 164-171. Article no. BJAST.2015.077. DOI: 10.9734/BJAST/2015/14356

[6] Obueh, H.O. and Odesiri-Eruteyan E. (2016). A Study on the Effects of Cassava Processing Wastes on the Soil Environment of a Local Cassava Mill. *J Pollut Eff Cont*, 4:4 DOI: 10.4176/2375-4397.1000177

[7] Izonfuo, W.A.L., Bariweni, P.A. and George, D.M.C. (2013). Soil contamination from cassava wastewater discharges in a rural community in the Niger Delta, Nigeria," *Journal of Applied Sciences and Environmental Management*, 17(1): 105–110.

[8] Dantas, M.S.M., Rolim, M.M., Duarte, A.S., França de Silva, E.F., Pedrosa, E.M.R and Dantas, D.C (2014). Chemical Attributes of Soil Fertilized with Cassava Mill Wastewater and Cultivated with Sunflower. *Scientific World Journal*, Article ID 279312, 10 pages http://dx.doi.org/10.1155/2014/279312

[9] Izah, S.C., Bassey, S.E. and Ohimain, E.I. (2018). Impacts of Cassava Mill Effluents in Nigeria. *Journal of Plant and Animal Ecology* 1(1): 15-42. *ISSN NO: 2637-6075 DOI:*10.14302/issn.2637-6075.jpae-17-1890

[10] Izah S.C., Enaregha, E.B. and Epidi, J.O. (2019). Changes in *in-situ* water characteristics of cassava wastewater due to the activities of indigenous microorganisms. *MOJ Toxicol.* 5(2):78–81. DOI: 10.15406/mojt.2019.05.00158

[11] Cumbana, A. Mirione, E., Cliff, J.J. and Bradbury, H. (2007). Reduction of cyanide content of cassava flour in Mozambique by the wetting method, *Food Chemistry*, 101: 894–897. doi:10.1016/j.foodchem.2006.02.062

[12] Jyothi, A.N., Sasikiran, K., Nambisan, B. and Balagopalan, C. (2005). Optimisation of glutamic acid production from cassava starch factory residues using Brevibacterium divaricatum. *Process Biochemistry* 40(11):3576-3579. DOI: 10.1016/j.procbio.2005.03.046

[13] Li, S., Lui, Y., Zhou, Y., Luo, Z., Liu, J. and Zhao, M. (2017), The Industrial Application of Cassava: Current Status, Opportunities and Prospects. *Journal of the Science of Food and Agriculture*: 97(8): 2282-2290. DOI: 10.1002/jsfa.8287.

[14] Burns, A.E., Glendow, R.M., Zacarias, A.M., Curambe, C.E., Miller, R.E. and Cavagnaro, T.R. (2012). Variations in the Chemical Composition of Cassava (*Manihot esculenta*, Crantz) Leaves and Roots as Affected by Genotypic and Environmental Variation. *J. Agric. Food Chem.*: 60(19), pp.4946-4956. DOI: 10.1021/jf2047288

[15] Pueyo, N., Miguel, N., Ovelleiro, J.L. and Ormad, M.P. (2016). Limitations of the removal of cyanide from coking wastewater by ozonation and by the hydrogen peroxide-ozone process. *Water Science & Technology* 74(2): 482-490. https://iwaponline.com/wst/article-pdf/74/2/482/460970/wst074020482.pdf

[16] Abdel-Aziz, M.H., Bassyouni, M., Gutub, S.A., El-Ashtoukhy, E.S.Z., Abdel-Hamid, S.M.S. & Sedahmed, G.H. (2016). Removal of Cyanide from Liquid Waste by Electrochemical Oxidation in a New Cell Design Employing a Graphite Anode. *Chemical Engineering Communications*, 203(8): 1045-1052, DOI: 10.1080/00986445.2015.1135796

[17] Abbas, M.N., Abbas, F.S. and Ibrahim, S.A. (2014). Cyanide Removal from Wastewater by Using Banana Peel. *Journal of Asian Scientific Research*, 4(5): 239-247

[18] Yeddou, A.R., Nadjemi, B., Halet, F., Ould-Dris, A. and Capart, R. (2010). Removal of cyanide in aqueous solution by oxidation with hydrogen peroxide in presence of activated carbon prepared from olive stones. *Minerals Engineering* 23:32–39 doi:10.1016/j.mineng.2009.09.009

[19] Volesky, B. (2007). Biosorption and me. *Water Research*. 41(18): 4017-4029; https://doi.org/10.1016/j.watres.2007.05.062

[20] Dash, R.R., Balomajumder, C. and Kumar, A., (2009). "Treatment of cyanide bearing water/Wastewater by plain and Biological Activated Carbon," *Ind. Eng. Chem. Res.*, 48(7), 3619-3627.

[21] Dwivedi, N., Balomajumder, C and Mondal P. (2016). Comparative investigation on the removal of cyanide from aqueous solution using two different bioadsorbents. *Water Resources and Industry*, Vol. 15, Pages 28-40. https://doi.org/10.1016/j.wri.2016.06.002

[22] Castro, J. Bonelli, P. Cerrella, E. and Cukierman, A. (2000). Phosphoric acid activation of agricultural residues and bagasse from sugarcane: influence of the experimental conditions on adsorption characteristics of activated carbons, De *Ind. Eng. Chem. Res*; 39, 4166-4170.

[23] De Gisi S., Lofrano, G., Grassi, M. and Notarnicola M. (2016). Characteristics and adsorption capacities of low-cost sorbents for wastewater treatment: A review. *Sustainable Materials and Technologies* (9), pp.10-40, http://dx.doi.org/10.1016/j.susmat.2016.06.002.

[24] Herawan, S.G., Hadi, M.S., Ayob, Md. R and Putra, A. (2013): Characterization of Activated Carbons from Oil-Palm Shell by CO_2 Activation with No Holding Carbonization Temperature. *The Scientific World Journal*.

[25] Poku, K., (2002). Small-Scale Palm Oil Processing in Africa.FAO Agriculture Services Bulletin 148, Food and Agricultural Organization of the United Nations, Rome, Italy.

[26] Prasertsan, S. and Prasertsan, P (1996): Biomass residues from palm oil mills in Thailand: an overview of the quantity and potential usage. *Biomass Bioenergy perspective*.11(5): 87-395.

[27] Singh, R.P., Hakimi, I.M and Esa, N (2010). Composting of waste from palm oil mill: A College, London. 190 Rajah Rasiah. Sustainable waste management practice. *Review in Environmental Science and Biotechnology*, DOI: 10.1007/s11157-010-9199-2.

[28] Parveen, F.R. Rajeev, P. Singh, H.I. M and Norizan, E. (2010): *World Applied Sciences Journal* 11 (1): 70-81.

[29] Anyanwu, C.N. (2013). Present and Prospective Energy Use Potentials of Selected Agricultural Wastes in Nigeria. *Journal of Renewable and Sustainable Energy*, 4-5.

[30] Ohimain, E., Izah, S. and Obieze, F. (2013). Material-mass balance of smallholder oil palm processing in the Niger Delta, Nigeria. *Advance J Food Sci Technol*, 5(3): 289-294.

[31] Ridzuan, R., Khan, M.M.R., Rosli, M. Y., Huei, R. O., Halim, R.M., Aziz, A.A., Zawawi, I. and Zainal, N.H. (2014). *In-Situ* Impregnation of Copper Nanoparticles on Palm Empty Fruit Bunch Powder. *Advances in Nanoparticles*, 3: 65-71. http://www.scirp.org/journal/anp http://dx.doi.org/10.4236/anp.2014.33009

[32] Ajayi, O.A., Olakunle, M.S., Edet, M.O., Dabai, F.N. and Eletta, O.A.A. (2017). Development and Application of Copper-Impregnated Oil Palm Fibre Ash as Adsorbent for Cyanide. *Umudike Journal of Engineering Technology (UJET)*, 3(2): 1-13.

[33] Suvash C.P., Mbewe P.B.K., Kong S.Y. and Šavija B. (2019). Agricultural Solid Waste as Source of Supplementary Cementitious Materials in Developing Countries. *Materials*, 12, 1112; doi:10.3390/ma12071112. www.mdpi.com/journal/materials

[34] Lawson-Wood, K. and Robertson, I. (2016). Water Analysis Using LAMBDA UV-Visible Spectrophotometers: Free Cyanide Determination. PerkinElmer, Inc. Waltham, MA 02451 USA (www.perkinelmer.com)

[35] Asadpour, R., Sapari, N.B., Isa, M.H and Kakooei, S (2016). Acetylation of oil palm empty fruit bunch fibre as an adsorbent for removal of crude oil. *Environ Sci Pollut Res Int.* 23(12):11740-50.

[36] ASTM D1102-84; ASTM E871-82; ASTM E872-82 (2013). Standard Test Method for Ash, Moisture and Volatile Matter Analyses in Particulate Wood Fuels, ASTM International, West Conshohocken, PA. www.astm.org.

[37] Abdelwahab, O., Nasr, S.M. and Thabet, W.M. (2017). Palm fibres and modified palm fibres adsorbents for different oils. *Alexandria Engineering Journal* 56; 749–755

[38] Tobi A.R., Dennis J.O., Zaid H.M., Adekoya A.A., Yar, A. and Usman F. (2019). Comparative analysis of physiochemical properties of physically activated carbon from palm bio-waste. *Journal of Material Research and Technology*, 8(5): 3688 - 3695. https://doi.org/10.1016/j.jmrt.2019.06.015

[39] Zarina, Y., Mustafa-Al Bakri, A.M., Kamarudin, H., Nizar, I.K. and Rafiza, A.R. (2013). Review on the various ash from palm oil waste as geopolymer material. *Rev. Adv. Mater. Sci*. 34, 37-43.

[40] Chua, S., Tan, C., Mirhosseini, H., Lai, O., Kamariah, L., & Baharin, B. (2009). Optimization of ultrasound extraction condition of phospholipids from palm-pressed fibre. *J. Food Eng.* 403–409.

[41] Shinoj, S., Visvanathan, R., Panigrahi, S., & Kochubabu, M. (2011). Oil palm fibre (OPF) and it's composite. A review. *Ind. Crop. Prod.*, 33, 7–22. doi:10.1016/j.indcrop.2010.09.009

[42] Depci, T. (2012). Comparison of activated carbon and iron impregnated activated carbon derived from Gölbasi lignite to remove cyanide from water. *Chemical Engineering Journal*, 181-182: 467-478. doi:10.1016/j.cej.2011.12.003

[43] Banerjee, S., Mukherjee, S., LaminKa-ot, A., Joshi, S.R., Mandal, T. and Halder, G. (2016). Biosorptive uptake of Fe^{2+}, Cu^{2+} and As^{5+} by activated biochar derived from *Colocasia esculenta*: Isotherm, kinetics, thermodynamics, and cost estimation. *Journal of Advanced Research* 7, 597–610.

[44] Yetilmezsoy, K., Demirel, S., Vanderbei R.J (2009). Response surface modelling of Pb (II) removal from aqueous solution by Pistacia vera L.: Box–Behnken experimental design. *Journal of Hazardous Materials*, 171(1–3):551–562.

[45] Gaurav D.G and Sharma, M.P. (2015). Application of Box–Behnken design in the optimization of biodiesel yield from Pongamia oil and its stability analysis. *Fuel* 145: 256–262 http://dx.doi.org/10.1016/j.fuel.2014.12.063

[46] Kumar, A., Prasad, B. and Mishra, I.M. (2008). Adsorptive Removal of Acrylonitrile Using Powdered Activated Carbon. *Journal of Environmental Protection Science:* Vol. 2:54 – 62.

[47] Wang, S-G., Dong-Bo, C., Yong-Wang, Li., Wang, J., and Jiao, H (2005). Chemisorption of CO_2 on Nickel Surfaces. *J. Phys. Chem. B*, 109, 40, 18956–18963. https://doi.org/10.1021/jp052355g

[48] Abia A.A. and Igwe J.C. (2005). Sorption kinetics and intra particulate diffusivities of Cd, Pb and Zn ions on maize cob. *African Journal of Biotechnology*. 04(6):509-512

[49] Girish, C.R and Murty, V.R (2016). "Mass Transfer Studies on Adsorption of Phenol from Wastewater Using *Lantana camara*, Forest Waste", *International Journal of Chemical Engineering*, vol. 2016, Article ID 5809505, 11 pages. https://doi.org/10.1155/2016/5809505

[50] Shahbeig, H., Bagheri, N., Ghorbanian, S. A., Hallajisani, A and Poorkarimi, S. (2013). A new adsorption isotherm model of aqueous solutions on granular activated carbon," *World Journal of Modelling and Simulation*, vol. 9, no. 4, pp. 243–254.

[51] Chan, L.S., Cheung, W.H., Allen, S.J., and McKay, G. (2012). Error analysis of adsorption isotherm models for acid dyes onto bamboo derived activated carbon," *Chinese Journal of Chemical Engineering*, vol. 20, no. 3, pp. 535–542.